Anal. Chem. **2002,** *74,* 1111−1118

Method for Measuring Oxygen Diffusion Coefficients of Polymer Films by Luminescence Quenching

Kristi A. Kneas,[†,‡] J. N. Demas,*[,†] Bryant Nguyen,[†] Aaron Lockhart,[†] Wenying Xu,[†] and B. A. DeGraff*[,§]

Department of Chemistry, University of Virginia, McCormick Road, Charlottesville, Virginia 22904-4319, and Department of Chemistry, James Madison University, Harrisonburg, Virginia 22807

To ascertain the relationship between the physical properties of polymer supports and the observed response of luminescence-based oxygen sensors, a quenching-based method was developed to measure oxygen diffusion in polymers. The method offers advantages over existing quenching-based techniques since it allows a simple correction for films of high optical density, and the computations do not assume uniform oxygen concentration throughout the film. Diffusion coefficients (*D*) were measured for a series of sensors with $[Ru(Ph_2phen)_3]Cl_2$ (Ph_2phen = 4,7-diphenyl-1,10-phenanthroline) as the luminophore and polystyrene, poly(trimethylsilylmethyl methacrylate), poly(butyl methacrylate), poly(trimethylsilylmethyl methacrylate-*co*-butyl methacrylate), or poly(trimethylsilylmethyl methacrylate-*co*-1*H*,1*H*-heptafluorobutyl methacrylate) as the support. The solvent from which the films were cast was varied, and filler materials such as hydrophobic, amorphous silica or tributyl phosphate plasticizer were added. Results are interpreted by a domain model in which the local environment of the sensor, rather than the bulk properties of the polymer, is the most critical parameter in sensor design.

With the continued wide use of polymer materials for diverse applications such as food containers, controlled drug-delivery systems, dental composites, sensor supports, separation materials, and medical implants,[1] molecular permeation through polymer films is an area of great interest. Specifically, diffusion, or the transfer of matter from one region to another as a result of random molecular motions, is important to many polymer applications. Fick's law, given in eq 1, is the quantitative expression for diffusion.

$$F = -D\partial C/\partial X \quad (1)$$

F is the rate of transfer per unit area, *D* is the diffusion coefficient (in cm^2/s); *C* is the concentration of diffusant, and *X* is the position measured normal to the film being permeated. For sensors, the rate of diffusion of the analyte determines the response time.[2,3]

Over the past decade, the use of polymer-supported luminescence-based oxygen sensors for industrial purposes has risen sharply. Applications range from the microscopic, in which oxygen concentration gradients are imaged in biological samples,[4,5] to the macroscopic, in which the pressure distribution is measured on the wing of an aircraft using pressure-sensitive paints (PSPs).[6,7] While the applications of luminescence-based oxygen sensors continue to increase in number, the fundamental understanding of oxygen sensors and factors governing their response remain uncertain. This is particularly true for combined sensor−support systems. As a result, the design of new materials with the exact performance characteristics for a given application remains a challenge. The complexity of luminescence-based oxygen sensors results primarily from immobilization of the dye, most commonly in a polymer support. Neither the detailed role of the polymer support in controlling the photophysical behavior of sensors nor the relationship between film fabrication and response is well understood despite the fact that the polymer support has a tremendous effect on sensor properties. Such information is critical to understanding the response times of sensors and the micromechanistic quenching details. To ascertain the relationship between physical properties of polymer supports and the observed response of luminescence-based oxygen sensors, an improved quenching-based method was developed to measure oxygen diffusion in polymers. Measurement of the diffusion coefficient gives an indication of the response time of the sensor.

Traditionally, permeation or sorption techniques have been utilized to measure diffusion coefficients in polymer films. For permeation measurements, a polymer sample is configured such that it creates a barrier between the diffusing gas and the appropriate detection system. The flow of the gas through the sample is monitored with time until steady-state conditions are

* To whom correspondence should be addressed: (e-mail) demas@virginia.edu; degrafba@jmu.edu.

[†] University of Virginia.

[‡] Current address: Division of Natural Sciences, Maryville College, Maryville, TN 37804.

[§] James Madison University.

(1) National Research Council Committee on Polymer Science and Engineering. *Polymer Science and Engineering: the shifting research frontiers*; National Academy Press: Washington, DC, 1994.

(2) Crank, J.; Park, G. S. Methods of Measurement. *Diffusion in Polymers*; Academic Press: London, 1968; pp 1−39.

(3) Crank, J. *The Mathematics of Diffusion*; Clarendon Press: Oxford, England, 1975.

(4) Hogan, M. C. *J. Appl. Physiol.* **1999**, *86*, 720−724.

(5) Zhao, Y.; Richman, A.; Storey, C.; Radford, N. B.; Pantano, P. *Anal. Chem.* **1999**, *71*, 3887−3893.

(6) Gouterman, M. *J. Chem. Educ.* **1997**, *74*, 697−702.

(7) Demas, J. N.; DeGraff, B. A.; Coleman, P. B. *Anal. Chem.* **1999**, *71*, 793A−800A.

10.1021/ac010867v CCC: $22.00
Published on Web 01/26/2002

reached. For sorption techniques, the diffusion coefficient is determined from the time dependence of gas absorption or desorption. Flow techniques have given the most reliable data, but saturation/outgassing techniques are much simpler and less expensive to apply. Additionally, saturation/outgassing techniques can be used for a much broader range of polymer samples, while flow techniques are limited to polymers that can be formed as films. The lack of established literature values and the lack of agreement for some reported values, however, indicate the inherent difficulties in using these methods to measure the diffusion coefficient. Modified methods are needed that allow accurate and rapid measurement of oxygen diffusion through polymer films. It will be demonstrated that, with the advent of improved instrumentation and detection schemes and mathematical analysis tools, it is possible to obtain reliable results using a sorption technique combined with luminescence quenching methods.[2,8−10]

In the current work, the approach was to monitor the time dependence of oxygen quenching of the emission intensity of an inorganic transition metal complex within a polymer film following a step change in the external oxygen pressure. By fitting the resultant intensity versus time profile to an appropriate diffusion model for the film configuration, an accurate measure of the diffusion coefficient for the polymer film was obtained. This method is an improvement over earlier methods.[11,12] The approach was successful, and the methodology and results are presented. We first provide a brief review of existing methods.

Several spectroscopic techniques that utilize oxygen quenching to determine the rate of oxygen diffusion through polymer films have been reported. In 1963, Czarnecki and Kryszewski observed a decrease in the radius of emission intensity in a naphthalene-doped cylindrical tube of poly(methyl methacrylate).[13] The effect was later exploited by Hormats and Unterleitner[14] and Shaw[15] in the quantitative determination of the oxygen diffusion coefficient for poly(methyl methacrylate) by monitoring oxygen quenching of an organic phosphorescence. Though successful, this detection scheme is limited to systems that exhibit triplet−triplet absorption or room-temperature phosphorescence.

Petrak[16] and Holland et al.[17] reported a modified flow-through technique in which a sensing film was placed between the membrane of interest and an impermeable substrate. The sensing film contained both a sensitizer that produced singlet oxygen upon excitation and a singlet oxygen scavenger for which absorbance decreased upon reaction with singlet oxygen. The diffusion coefficients were determined from the absorbance measured as a function of time. Unfortunately, the method requires a complicated sample preparation and experiment times of hundreds of minutes.

Gao and Ogilby[18] introduced a technique in which the singlet molecular oxygen that was formed upon oxygen quenching of meso-tetraphenylporphine in polystyrene sheets was monitored via time-resolved near-infrared phosphorescence of the singlet oxygen formed. Though novel and able to produce accurate results, the technique requires a specialized instrument with a detection system sensitive to beyond 1 μm; it is, therefore, impractical for use with conventional instrumentation.

Experimentally, the method described here resembles that described by Cox,[19] Cox and Dunn,[20] Nowakowska et al.,[21] MacCallum and Rudkin,[22] and Guillet and Andrews,[23] in which oxygen quenching methods were exploited to measure the diffusion coefficient of oxygen in planar sheets of poly(dimethyl siloxane),[19] filled poly(dimethyl siloxane) samples,[20] polystyrene,[21−23] and poly(methyl methacrylate).[21] The approach was to monitor oxygen quenching of a fluorophore, which was believed to be homogeneously dispersed within the films, as a function of time. The fluorophores were all organic dyes.[19−23] Alternatively the quenching of excimers of polystyrene was monitored.[22] The mathematical determination of D varied, but a single underlying assumption in all cases was that the time-dependent emission intensity measured during the experiment corresponded to the average oxygen concentration throughout the film. In fact, in most cases, the intensity versus time curve was converted to a concentration versus time curve using the Stern−Volmer relationship.[19,20,23] Under some experimental conditions, this analysis is flawed, since the Stern−Volmer plot is measured under steady-state conditions when oxygen is distributed evenly throughout the film. Under step or dynamic conditions, the oxygen concentration determined from the steady-state Stern−Volmer quenching plot does not always accurately represent the average oxygen concentration in the film since the quenching does not linearly depend on concentration. Clearly, as oxygen diffuses through the film with time, the distribution of oxygen through the film changes and the measured intensity will not necessarily correspond to the value obtained under steady-state conditions.[11,12]

Mills and co-workers examined in detail the time response of planar oxygen sensors to step changes in analyte.[11] Using a diffusion model with no approximations, they quantitatively accounted for the large differences in behavior for step increases and step decreases in the analyte concentration. They did not use this model for evaluating diffusion coefficients, although the mathematical machinery was appropriate.

The Mills' approach was then elegantly developed for measurement of diffusion coefficients by Yekta et al.[12] The authors provided the equations for diffusion and quenching in planar films exposed to analyte on either one or both faces. They provide equations for both diffusion in to and out of the film for a step change in the analyte concentration. Both theoretical and experi-

(8) Shelby, J. E. Permeation, Diffusion, and Solubility Measurements. In *Handbook of Gas Diffusion in Solids and Melts*; Shelby, J. E., Ed.; ASM Int.: Materials Park, OH, 1996; pp 1−13.
(9) Shelby, J. E. Molecular Solubility and Diffusion. In *Treatise on Materials Science and Technology*; Tomozawa, M., Doremus, R. H., Eds.; Academic Press: New York, 1979l Vol. 17, pp 1−40.
(10) Shelby, J. E. Gas Diffusion Measurements in Glasses. In *Experimental Techniques of Glass Science*; Simmons, C. J., El-Bayoumi, O. H., Eds.; American Ceramics Society: Westerville, OH, 1993; pp 363−381.
(11) Mills, A.; Chang, Q. *Analyst* **1992**, *117*, 1461−1466.
(12) Yekta, A.; Masoumi, Z.; Winnik, M. A. *Can. J. Chem.* **1995**, *73*, 2021−2029.
(13) Czarnecki, S.; Kryszewski, M. *J. Polym. Sci. A* **1963**, *1*, 3067−3077.
(14) Hormats, E. I.; Unterleiner, F. C. *J. Phys. Chem.* **1965**, *69*, 3677−3681.
(15) Shaw, G. *Trans. Faraday Soc.* **1967**, *63*, 2181−2189.
(16) Pertrak, K. *J. Appl. Polym. Sci.* **1979**, *23*, 2365−2371.
(17) Holland, R. V.; Rooney, M. L.; Santangelo, R. A. *Die Angew. Makromol. Chem.* **1980**, *88*, 209−221.
(18) Gao, Y.; Ogilby, P. R. *Macromolecules* **1992**, *25*, 4962−4966.
(19) Cox, M. E. *J Polym. Sci.* **1986**, *24*, 621−636.
(20) Cox, M. E.; Dunn, B. *J. Polym. Sci.* **1986**, *24*, 2395−2400.
(21) Nowakowska, M., Najbar, J.; Waligóra, B. *Eur. Polym. J.* **1976**, *12*, 387−391.
(22) MacCallum, J. R.; Rudkin, A. L. *Eur. Polym. J.* **1978**, *14*, 655−656.
(23) Guillet, J. E.; Andrews, M. *Macromolecules* **1992**, *25*, 2752−2756.

mental data are provided. The theory makes several assumptions that, while appropriate for their systems, are not always satisfied. They assume the quenching is accurately described by a linear Stern−Volmer equation and that the optical density is low enough that the sample is uniformly excited. These are issues that we will deal with in the current paper. They give a nice historical background and explain the limitations of previous quenching based techniques.

The primary differences between our approach and those previously reported are the use of a highly stable luminescent transition metal complex, as opposed to an organic fluorophore, and properly accounting for the quenching properties as a function of the nonuniform oxygen concentration during equilibration. Also, while the standard experimental approach assumes uniform excitation throughout the films, the method described here allows easy correction for the high optical density of films in which the exciting light is attenuated across the film. It also easily handles the problem of nonlinear Stern−Volmer plots.

EXPERIMENTAL SECTION

Materials. The monomers butyl methacrylate (BMA, Aldrich), trimethylsilylmethyl methacrylate (TMSMMA, United Chemical Technologies), and 1*H*,1*H*-heptafluorobutyl methacrylate (F-BMA, PolySciences) were used as received as were polystyrene (MW = 280 000, Aldrich), benzoyl peroxide (BPO, Aldrich), dichloromethane and trichloroethane (Mallinckrodt), bathophenanthrolineruthenium chloride, $[Ru(Ph_2phen)_3]Cl_2$ (Ph_2phen = 4,7-diphenyl-1,10-phenanthroline; G. Frederick Smith), hydrophobic, amorphous TS720 silica (Cab-O-Sil), and tributyl phosphate plasticizer (TBP, Aldrich).

Polymer Synthesis. All monomers were polymerized by radical initiation using BPO to form homopolymers or copolymers of trimethylsilylmethyl methacrylate and butyl methacrylate (30 mol %) or trimethylsilylmethyl methacrylate and F-BMA (30 mol %). Bulk polymerizations were carried out under nitrogen with the monomer(s) and initiator (0.3−0.8 wt % by mass of monomer) in a septum-capped test tube. A needle attached to a nitrogen-filled balloon was inserted into the septum. Temperature steps were 55 °C for 2 h, 70 °C for 6 h, and 90 °C for 2 h. The polymer or copolymer was redissolved in CH_2Cl_2 and precipitated in methanol/CH_2Cl_2 (20:1, v/v).

For the current work, information such as molecular weight and polydispersity were not relevant. With the exception of the plasticized films, all polymers were below their T_g. For all the polymers synthesized in-house, there were no significant differences in oxygen sensor response and quality of the cast films between different batches of the same polymers.

Sample Preparation. Thin polymer films were prepared by casting solutions of the polymer (5 wt %) with the metal complex (10^{-3}−10^{-4} M) dissolved in dichloromethane or a 1:1 mixture of dichloromethane/trichloroethane into a Teflon well on a window used in the sample chamber. A small amount of solvent was evaporated to obtain a viscous solution prior to casting. Filler materials such as silica and TBP were added in appropriate amounts based on weight percent filler relative to polymer to the mixture prior to casting. For example, 0.1 g of filler to 1 g of polymer is reported as 10 wt %. After the solvent evaporated, films were carefully cut from the Teflon mold and stored in the dark prior to use. Prior to measurements, films were outgassed under vacuum in the sample chamber for a period of at least 20−30 min to ensure evaporation of residual solvent. Reproducible results confirm that all the solvent was removed on the first evacuation.

Diffusion measurements required that oxygen permeate only one surface of the film, so cast films were discarded if they became detached from the window. To further ensure that lateral diffusion did not affect results, a small region in the center of the films was masked off for measurement using black tape on the opposite side of the window from the sample.

Stern−Volmer Quenching Plots. Emission spectra were recorded on a double-monochromator Spex Fluorolog 2+2 spectrofluorometer using front face detection. Intensity-based Stern−Volmer plots were acquired by measuring the emission spectra at different oxygen partial pressures in a vacuum-tight system. The pressure was monitored using a Paroscientific Portable Standard Digiquartz pressure sensor, model 740-30A (0.01% accuracy). Variations during the course of a measurement were observed to be in the ∼0.01−0.09 Torr range. Excitation was at 450 nm, near the maximum wavelength of the MLCT absorption band, and the intensity at the emission maximum (605−620 nm) was recorded for each oxygen pressure. Oxygen quenching sensitivity, S, was calculated from eq 2.

$$S = I_0/I_{ox} - 1 \qquad (2)$$

The intensities I_0 and I_{ox} were measured in the absence of quencher and in 1 atm of oxygen, respectively.

Instrumentation and Data Acquisition. The front surface viewing configuration was used on the fluorometer for measuring the diffusion coefficients. The excitation was normal to a sample film bound tightly to a quartz window in an evacuable chamber. A gas reservoir was attached to the sample portion of the cell with a valved stem. The reservoir could also be sealed off with a valve from the sample compartment. The sample compartment and reservoir were evacuated before closing the valve between the two chambers. The reservoir was then filled with the desired amount of oxygen, and the valve to the gas-handling system was closed to isolate the entire apparatus from the vacuum pump and gas cylinder. The intensity was monitored for a short period (60−90 s) under the initial conditions to ensure signal stability, and the valve between the two chambers was opened to produce a step change in the oxygen pressure. The intensity at the maximum emission wavelength was monitored with time by employing SPEX Datamax software in the time-based mode. Time intervals of 0.1, 0.5, or 1 s were selected depending on the magnitude of the expected diffusion rate; more points were collected for faster diffusion rates.

As oxygen diffused through the planar film and quenched the emission intensity of the ruthenium complex with the step change from vacuum to a high pressure of oxygen, the intensity decreased as shown in Figure 1. A plateau was reached once oxygen diffused through and equilibrated in the film. The data recorded before the step change provided an unquenched reading. The initiation of the decay was taken at the instant the pressure was changed. The intensity at $t = 0$ was approximated from the average intensity prior to the step change.

A thermistor-based digital temperature probe (Radio Shack) was used to monitor temperatures. Experiments were carried out

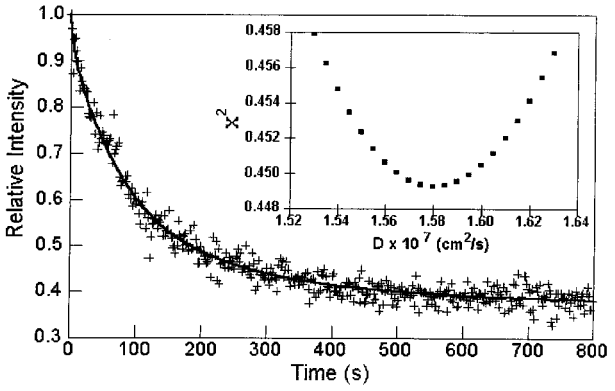

Figure 1. Typical emission intensity versus time curve for [Ru(Ph_2-phen)$_3$]Cl_2 in polystyrene cast from 50:50 dichloromethane/trichloroethane (The +'s are the experimental data, and the solid line is the best fit to the diffusion model.) and χ^2 plot (inset) used to determine D ($D = 1.58 \times 10^{-7}$ cm^2/s for this run.).

at room temperature, 25 ± 2 °C. The small difference in temperature between sample runs did not produce a measurable change in the diffusion coefficient given the limits of detection of this technique. The temperature in the chamber was observed to remain constant within 0.1 °C during the course of diffusion measurements.

The optical densities of sample films were determined using a Hewlett-Packard 8452A diode array spectrophotometer. Polymer blank corrections were made in the following manner: an air measurement was used for the instrument blank; a region of the film, much smaller than the aperture of the sample holder, was masked off for measurement using black tape; the absorption spectrum was acquired; and the optical densities at the wavelength of excitation (450 nm) and a wavelength at which the ruthenium complex does not absorb (800 nm) were recorded. The polymer blank-corrected optical density was determined by subtracting the optical density at 800 nm from that measured at 450 nm. Five measurements were averaged to improve accuracy of the determination. Film thicknesses were measured using a digital micrometer with an uncertainty of 0.01 mm.

Data Analysis. Data were fit to an equation describing the emission intensity as a function of time. The observed intensity versus time is proportional to the integrated emission intensity over the entire thickness of the film and is given by

$$I_{\text{total}}(t) = \int_0^1 I(X,t)\, \mathrm{d}X \tag{3}$$

where the film thickness is normalized to 1, X corresponds to the position within the film, and t corresponds to time. The assumptions made were that the luminophore was doped uniformly and that quenching properties were uniform throughout the film. Further, the excitation was assumed to be uniform throughout the sample. For higher optical density films, the last assumption was not valid and an additional correction was applied (vide infra).

For the oxygen sensor films used in these studies, the intensity in eq 3 depends on oxygen concentration and is given at each depth element in the film by the Stern−Volmer expression for nonlinear quenching. Two mathematically equivalent models for describing nonlinear quenching curves are the nonlinear gas solubility model[24] and the two-site quenching model.[25,26] Since the nonlinear solubility model is a little simpler mathematically, it was used. Using this model, $I(X,t)$ is given by

$$I(X,t) = \frac{I_0}{\left(1 + A[\mathrm{O_2}] + \dfrac{B[\mathrm{O_2}]}{1 + b[\mathrm{O_2}]}\right)} \tag{4}$$

I_0, the intensity in the absence of oxygen, was normalized to 1 to simplify the calculations. A, B, and b are fitting parameters, and no physical significance was ascribed to them.

The oxygen concentration (or partial pressure) given in eq 4 can be determined using an appropriate equation for diffusion in an infinite plane sheet. A uniform initial distribution of oxygen, C_0, within the film and a constant oxygen concentration, C_1, at the film's surface during the experiment are assumed. It is also assumed that the film is attached on one side to an impermeable surface. The appropriate expression for all times, which has been modified to account for normalization of film thickness, is

$$\frac{C - C_0}{C_1 - C_0} = 1 - \frac{4}{\pi}\sum_{n=0}^{\infty}\left(\frac{(-1)^n}{2n+1}\right) \times \exp\left(\frac{-D(2n+1)^2\pi^2 t}{4l^2}\right)\cos\frac{(2n+1)\pi X}{2} \tag{5}$$

where X is the normalized depth (0−1) given by x/l and l and x are the actual thickness and position in the film, respectively. Alternatively, an expression that can be used for small times is given by

$$\frac{C - C_0}{C_1 - C_0} = \sum_{n=0}^{\infty}(-1)^n \operatorname{erfc}\frac{(2n+1)l - Xl}{2(Dt)^{1/2}} + \sum_{n=0}^{\infty}(-1)^n \operatorname{erfc}\frac{(2n+1)l + Xl}{2(Dt)^{1/2}} \tag{6}$$

C is the oxygen concentration, or in this case the partial pressure, within the film; D is the diffusion coefficient (in cm^2/s); erfc is 1 minus the error function; l is the film thickness (in cm); and t is the time (in s).[2,3]

On the time scale of the measurements described here, eq 6 proved to give an accurate description of oxygen diffusion and avoided the oscillatory behavior and poor convergence in Mathcad of eq 5. It was used for all measurements reported. Rearrangement of eq 6 to solve for C gives eq 7

$$C = \left[\sum_{n=0}^{\infty}(-1)^n \operatorname{erfc}\frac{(2n+1)l - Xl}{2(Dt)^{1/2}} + \sum_{n=0}^{\infty}(-1)^n \operatorname{erfc}\frac{(2n+1)l + Xl}{2(Dt)^{1/2}}\right](C_1 - C_0) + C_0 \tag{7}$$

For the special case of $C_0 = 0$ (i.e., initially a vacuum as used in this work), eq 7 is greatly simplified.

Substitution of eq 7 into the Stern−Volmer expression (eq 4) for the oxygen concentration, and further substitution into eq 3 gave the final equation for integration. During integration, a discontinuity at time $t = 0$ when eq 6 was used required that the intensity be assigned. When the initial oxygen concentration, C_0, was equal to zero, no quenching occurred; the intensity at $t = 0$ was equal to the maximum intensity, I_0, which was normalized to 1.

Experimental data were fit to eq 3 using a grid search nonlinear least-squares fitting. The diffusion coefficient was the only variable, and the chi-square parameter, χ^2, was calculated from

$$\chi^2 = \sum_{T=0}^{T_{\text{final}}} (I_{\text{total}}(T,D) - I_{\text{exp}})^2 \tag{8a}$$

$$\chi_r^2 = \chi^2 / N \tag{8b}$$

χ^2 was minimized to find the diffusion coefficient that produced the best fit to the experimental data. The summation was carried out over the N points from time 0 to a terminal time taken shortly after the intensity plateau was reached. For comparisons between fits using a different number of points, the reduced chi-square, χ_r^2, was calculated using eq 8b. With a single parameter fit of this equation there are no false minimums, and by making plots of the χ_r^2 versus D, one gets a clear idea of the precision of the measurement.

To achieve reasonable signals for measurements, it was necessary to dope some sensor films at relatively high levels. For optical densities greater than 0.1, the assumption of uniform excitation throughout the sample was invalid. At higher optical densities, a disproportionate amount of emission intensity came from the portion of the film nearest the window that oxygen reached last. It was necessary to account for the effect when the theoretical curves for data fitting were generated. An attenuation factor was multiplied by the intensity so that eq 3 became

$$I_{\text{total}}(T) = \int_0^1 (10^{-\text{OD}\,X} I(X,T))\, \mathrm{d}X \tag{9}$$

where OD is the measured optical density of the sample film at the excitation wavelength.

The best-fit Ds were relatively insensitive to the choice of l. A 5% uncertainty in l yielded an 8% uncertainty in D.

RESULTS AND DISCUSSION

Measurement of *D* for a Known Sample. Figure 1 shows a typical intensity versus time curve for polystyrene cast from a 50:50 (v/v) solvent mixture of dichloromethane and trichloroethane. The solid line represents the best fit to the diffusion model. Results for the measurement of two separate polystyrene films are shown in Table 1 along with reported literature values. The precision of replicate measurements on the same sample is excellent as given by the standard deviation for each film. These uncertainties are also consistent with the narrowness of the χ_r^2 versus D plot that indicates the reproducibility of measurements on the same sample and of the experimental method. There is some variation in Ds obtained for the two different films as might be expected for completely different preparations but the differences are larger than we would expect on the basis of the uncertainties in film thicknesses. Different cast films are expected to have minor variations in polymer morphology that should produce variations in D. Ignoring the obvious outlier, the literature values are 2.3 ± 0.9 that compare quite well with our data.

Table 1. Measurement of *D* for Two Polystyrene Samples[a]

sample	thickness (cm)	OD	S	D ($\times 10^7$ cm^2/s)	χ_r^2 ($\times 10^4$)
PS	0.009	0.117	2.1	3.03 ± 0.04	2.7
PS	0.011	0.175	1.8	1.59 ± 0.01	4.6
PS mean				2.3 ± 0.8	
PS literature values[a]				1.1×10^{-8} [22]	
				1.1×10^{-7} [28]	
				2.3×10^{-7} [18]	
				2.8×10^{-7} [23]	
				3.1×10^{-7} [21]	

[a] Reported literature values are included for comparison.

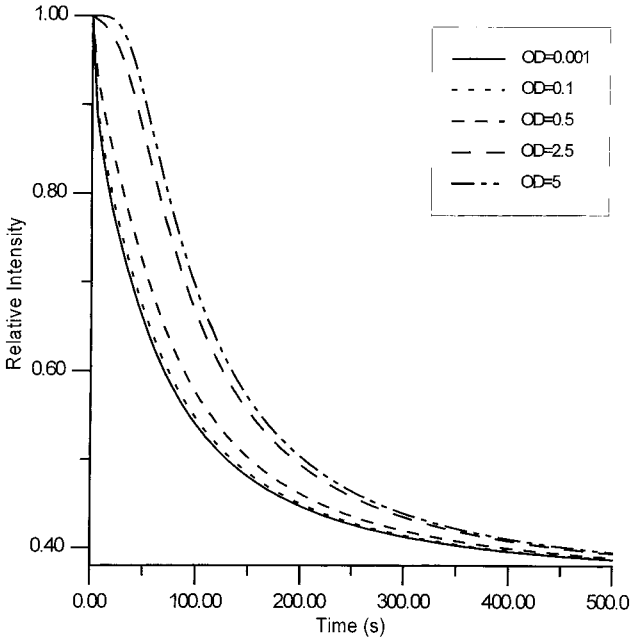

Figure 2. Simulations for optical density effects on intensity versus time curves.

Optical Density Correction. To obtain a reasonable signal-to-noise ratio, a high dye concentration was sometimes required for which the optical density was greater than ~0.05, the optically dilute limit. Under conditions in which the sample is not optically dilute, excitation does not occur uniformly through the film and the theoretical curve, based on eq 3 and uniform sample excitation, is not valid. Though optical densities of samples used in this study did not exceed 0.7, simulations are shown in Figure 2 for optical densities ranging from 0.001 to 5.0. For the simulations, a thickness of 0.01 cm, a D of 2.1×10^{-7} cm^2/s, and quenching parameters for $[Ru(Ph_2phen)_3]Cl_2$ in polystyrene were assumed.

(24) Li, X. M.; Wong, K. Y. *Anal. Chim. Acta* **1992**, *262*, 27.
(25) Demas, J. N.; DeGraff, B. A.; Xu, W. *Anal. Chem.* **1995**, *67*, 1377−1380.
(26) Carraway, E. R.; Demas, J. N. *Anal. Chem.* **1991**, *63*, 332−336.

Table 2. Errors in Diffusion Coefficient Resulting from High Optical Density

OD	calculated D ($\times 10^7$ cm^2/s)	χ_r^2	error ($\times 10^7$ cm^2/s)	% error
0.001	2.10	1.6×10^{-6}	−0.00	0.0
0.01	2.09	4.1×10^{-5}	−0.01	−0.5
0.05	2.05	0.0042	−0.05	−2.4
0.10	2.00	0.0010	−0.10	−4.8
0.25	1.87	0.027	−0.23	−11.0
0.50	1.70	0.11	−0.40	−19.0
0.75	1.56	0.24	−0.54	−25.7
1.0	1.46	0.40	−0.64	−30.5
2.5	1.18	1.4	−0.92	−43.8
5.0	1.08	2.0	−1.02	−48.6

Table 3. Measured Diffusion Coefficients for PTMSMMA Cast from Different Solvents

solvent	thickness (cm)	OD	S	D ($\times 10^6$ cm^2/s)	χ_r^2 ($\times 10^4$)
CH_2Cl_2	0.011	0.22	9.9	1.22 ± 0.01	2
	0.020	0.56	9.2	1.2 ± 0.2	0.5
mean				1.2 ± 0.1	
CH_2Cl_2/CH_3CCl_3, 1:1	0.017	0.16	6.0	3.96 ± 0.04	0.7
	0.017	0.23	6.5	2.14 ± 0.11	3.5
	0.024	0.65	6.9	2.63 ± 0.12	0.9
	0.033	0.43	7.2	2.35 ± 0.25	0.9
mean				2.8 ± 0.8	

Table 4. Measured Diffusion Coefficients for PTMSMMA Films Containing Silica (S) and Tributyl Phosphate Plasticizer (TBP)

sample	thickness (cm)	OD	S	D ($\times 10^6$ cm^2/s)	χ_r^2 ($\times 10^4$)
pTMSMMA			6.0−7.2	2.8 ± 0.8	
pTMSMMA + 2 wt % silica	0.034	0.40	6.8	2.45 ± 0.04	0.7
pTMSMMA + 8 wt % silica	0.017	0.38	7.6	1.47 ± 0.03	0.9
pTMSMMA + 25 wt % TBP	0.039	0.36	2.9	7.88 ± 0.05	10

The 0.001 curve is visually indistinguishable from the 0.10 curve. At very high optical densities, a lag time is observed before the luminescence intensity decreases. The lag time results because excitation and detection occur at the opposite side of the film from where oxygen is introduced. In the extreme case of very high optical density, excitation is very near the window and no quenching is observed until oxygen can diffuse through the entire thickness of the film. This results in the initial plateaus seen in the figure.

To assess the errors that would result by failure to account for the optical density, we fit the data of Figure 2 to eq 3. Table 2 shows the errors in D and the reduced χ_r^2 obtained for the different fits. Failure to correct for the optical density results in an underestimate of the diffusion coefficient, although the theoretical curve and calculated diffusion values are reasonable and have errors of less than 5% for optical densities up to 0.1. The significant errors observed for higher optical densities indicate the need for a correction. The χ_r^2 values and the shape of the theoretical intensity versus time curves do not become obviously distorted until the optical density exceeds 1. This demonstrates the potential for failing to recognize the effect. With visual inspection, the best-fit data up to an optical density of 0.25 are indistinguishable from the theoretical data, but theoretical fits for optical densities of 0.5 and greater are likely to give a clear indication that the model is no longer valid if the data are not too noisy.

For the work reported here, the optical density was measured for all films, and corrections were made with eq 9 as required. It is not clear whether this correction was necessary for measurements reported in the literature. Further, literature methods that employ the average concentration versus time curve do not allow a simple correction to be made. The ability to easily correct for optical density is a great advantage of our method.

Effects of Solvent on *D*. During sample preparation, it was discovered that films cast from a 1:1 (v/v) solvent mixture of dichloromethane/trichloroethane were more easily cut from the Teflon mold without detaching the sample film from the window. A different solvent system, however, is likely to have an effect on the diffusion coefficient as is demonstrated in Table 3 for the measurement of pTMSMMA films cast from dichloromethane and a 1:1 dichloromethane/trichloroethane solvent mixture. In the table, we show the mean and standard deviations where more than one experiment was performed.

Values of D obtained for pTMSMMA are reproducible and are significantly greater than those measured for polystyrene. This is not surprising given the likely increase in void volume resulting from the bulky trimethylsilyl group. The value of D obtained for films cast from the solvent mixture, 2.8×10^{-6} cm^2/s, is significantly greater than that obtained for films cast from dichloromethane only, 1.3×10^{-6} cm^2/s, probably as a result of the fact that the solvent mixture is a poorer solvent for the polymer. Because a poorer solvent results in the production of films with greater void volume and less organization of the polymer chains, an increase in the diffusion coefficient is, in general, observed. The significant dependence of diffusion coefficient on solvent system may account in part for the large variations in Ds found in the literature. Further, it demonstrates the subtle and critical role of solvent in film preparation.

Despite the observed increase in D, oxygen quenching sensitivity (S) was poorer for films cast from the solvent mixture. This was a surprising result, since one would expect a greater solubility and, hence, greater oxygen quenching for films with an increased void volume. It is possible that the metal complex is able to partition into domains in which the oxygen solubility and D are smaller and it is less efficiently quenched. The measured D represents the bulk response, but it is certainly possible for domains of varying oxygen diffusion and solubility properties to be present within the polymer films. Of further interest was the suggestion that S improves with increasing film thickness. This might be due to subtle differences in evaporation times.

Effects of Filler Materials on *D*. A series of measurements were carried out to determine D for films prepared with hydrophobic, amorphous silica filler and with TBP plasticizer. The results are shown in Table 4 for pTMSMMA films cast from a 1:1 dichloromethane/trichloroethane mixture. It was uncertain whether the addition of silica would result in an increase or decrease in D, but the results presented in Table 4 show a roughly 2-fold decrease in D with increasing amounts of silica. The decrease in

Table 5. Summary of Results for a Series of TMSMMA, BMA, and F-BMA Homopolymers and Copolymers with and without 5 wt % Silica Cast from CH_2Cl_2

sample	thickness (cm)	OD	S	D ($\times 10^6$ cm^2/s)	χ_r^2 ($\times 10^4$)
pBMA	0.012	0.09	2.8	1.93 ± 0.03	0.8
pBMA+silica	0.019	0.11	3.3	1.80 ± 0.02	1.4
pTMSMMA			9.6	1.2 ± 0.2	
pTMSMMA-*co*-BMA	0.010	0.24	4.7	1.04	0.2
			4.1 (aged)[a]	1.00 ± 0.02 (aged)[a]	0.4
pTMSMMA-*co*-BMA + silica	0.010	0.07	5.7	2.3 ± 0.1	1.2
			2.9 (aged)[a]	3.1 ± 0.2 (aged)[a]	3.6
pTMSMMA-*co*-FBMA	0.009	0.24	9.8	1.54	3.56
			5.8 (aged)[a]	1.97 (aged)[a]	3.76
pTMSMMA-*co*-FBMA[b]	0.012	0.34	7.8 (aged)[a]	1.23±.01 (aged)[a]	7
			7.0 (aged)[a]	0.98±.01 (aged)[a]	4.5
pTMSMMA-*co*-FBMA + silica	0.011	0.06	10.9	2.25	1.40
			6.0 (aged)[a]	2.16 (aged)[a]	2.23

[a] Data obtained after an elapsed time of at least 30 days. [b] Second film prepared from same batch of polymer.

D is a result of the strong adsorption of oxygen onto the silica particles that has been previously reported.[27] Hydrophobic amorphous silica has a very large surface area and acts to trap the oxygen; thus, the observed *D* is lower than that obtained for the unfilled polymer.

While *D* changed significantly on adding silica, *S* was at best minimally affected even up to 8% silica. This result suggests that the sites occupied by the metal complex are unaffected by the addition of silica. The local quenching environment and solubility near the complex are unaffected.

The addition of TBP produced the expected effect of increasing *D*. Plasticizers decrease the cohesive forces between polymer chains and allow greater segmental motion and, thus, more rapid diffusion of oxygen.[28] Not shown is the fact that TBP samples were extremely irreproducible to manufacture. We frequently obtained curves where the emission intensity plunged in the first few points and then showed more normal behavior. The source of this behavior is unknown but probably represents gross nonuniformities in the sensor distribution. The one reported result is for a film that gave a reasonable fit. Based on the difficulties of producing homogeneous mixtures for casting, this is a plausible explanation. Regardless, it is apparent that *S* was significantly degraded with the addition of TBP. Although it is possible that the decrease in *S* resulted from a decrease in oxygen solubility within the polymer film, we consider this unlikely because of the very large decrease in bulk solubility necessary to explain our results. We think the most likely possibility is that the metal complex is partitioned into domains of poorer oxygen diffusion than the bulk film.

Copolymers That Exhibit Degradation in *S*. In a study by Morin et al.,[29] fluorinated methacrylate supports gave much greater quenching response than their nonfluorinated analogues when doped with $[Ru(Ph_2phen)_3]Cl_2$. This is a result of the fact that fluorine derivatives are known to have excellent oxygen transport properties. The disadvantage of such polymer systems, however, is the increased monomer expense and the poor solubility and optical clarity (cloudiness) of polymer films with increasing fluorine content. It was of interest to determine whether copolymers of fluorinated methacrylates and TMSMMA might exhibit enhanced response characteristics and improved optical and dye solubility properties. Synthesis of copolymers would require less of the expensive fluorinated monomers and should give films of better optical quality and oxygen quenching.

Poly(TMSMMA-*co*-F-BMA) and poly(TMSMMA-*co*-BMA) were measured with and without 5 wt % hydrophobic amorphous silica. The polymers were easily dissolved and cast into optically transparent films. The homopolymer of F-BMA was not soluble and as such was not studied. The *S* values are given in Table 5 along with the measured responses of the homopolymers. The shapes of the Stern−Volmer plots were the same with reasonable linearity. As hoped, the initially measured response of pTMSMMA-*co*-F-BMA was better than that of pTMSMMA. Adding silica improved the sensitivity of all polymers, but especially the homopolymer. Not surprisingly, the response for pTMSMMA-*co*-BMA fell between that of pTMSMMA and pBMA.

Once again we find that there is poor correlation between *S* and *D*. Addition of silica can affect both these quantities, but there are no obvious trends. Clearly, aging can degrade quenching performance. This is especially true for the systems containing fluorinated components with decreases in *S* of over a factor of 2. We initially suggested that the copolymers were reorienting with time to produce a more ordered structure; increased order should reduce void volume and lower *D*. If that assumption is correct, the *D*s should decrease with time along with *S*. Clearly, this explanation is incorrect. For p(TMSMMA-*co*-F-BMA) with silica, *D* actually increases as *S* drops precipitously. For the other copolymers, the discrepancies are less, but *D* consistently increases or remains essentially unchanged with aging while *S* falls.

No general trend was observed for the change in *D* with film aging. Possible interpretations are that oxygen solubility may be decreasing with time or microcrystallinity of the metal complex is increasing. Either would result in a reduction in *S*. Alternatively, with time, the metal complex may be migrating to domains in which it is less heavily quenched. Without further morphology studies, we cannot distinguish between these possibilities, though

(27) Carraway, E. R. Excited-State Quenching of Immobilized Ruthenium (II) Complexes. Ph.D. Dissertation, University of Virginia 1981.

(28) Pauly, S. Permeability and Diffusion Data. In *Polymer Handbook*, 2nd ed.; Brandrup, J., Immergut, E. H., Eds.; John Wiley & Sons: New York, 1999; pp 435−445.

(29) Morin, A. M.; Xu, W.; Demas, J. N.; DeGraff, B. A. *J. Fluoresc.* **2000**, *10*, 7−12.

we believe that microcrystallization of the metal complex is the most unlikely interpretation. Fluorescence microscopic investigations of other sensors with $[Ru(Ph_2phen)_3]Cl_2$ as the luminophore reveal no propensity for microcrystal formation in the polar or hydophobic polymer supports that have been investigated.[30,31]

A second surprise was the larger *D* measured for pBMA compared to pTMSMMA, especially given the poorer quenching sensitivity of pBMA relative to pTMSMMA. A much greater void volume is expected for pTMSMMA as a result of the bulky trimethylsilyl group, and thus, greater *D*s were expected. A possible interpretation is that dichloromethane is a poorer solvent for pBMA than for pTMSMMA. Since a poorer solvent yields a film with less order and an increased void volume, a greater *D* would be observed. This possibility is supported by the fact that, when cast from a poorer solvent (1:1 dichloromethane/trichloroethane solvent mixture), pTMSMMA gave a diffusion coefficient (2.8×10^{-6} cm^2/s) that is greater than the diffusion coefficient reported for pBMA in Table 5.

On comparing *D* obtained for pTMSMMA-*co*-BMA and for the two homopolymers, pTMSMMA and pBMA, it is apparent that *D* was lower in the copolymer than the homopolymers. This is an interesting result, because one might expect the copolymer to have a less organized structure with a greater void volume. Though unlikely, it is possible that the solvent system is poorer for the homopolymers than for the copolymer. No other interpretation can be offered at this time. A larger *D* was measured for pTMSMMA-*co*-F-BMA than for pTMSMMA. This result is not surprising, since the fluorinated homopolymer, though not measured here, is likely to have a very large diffusion coefficient.

The measured *D*s also provided some extremely useful information in terms of the relationship between the macroscopic diffusion and the measured quenching sensitivity of sensor films. It was found that many factors such as solvent, fillers, aging of films, etc., dramatically affected both the quenching sensitivity and the diffusion; but the surprising result was that the same general trends were not observed for *S* and *D*. That is, the oxygen quenching response did not track the measured diffusion coefficient as expected. Indeed, the failure to find consistent patterns of quenching behavior that track changes in bulk polymer properties provides further evidence for the domain model suggested earlier.[32] It seems likely that the metal complex is able to partition into various regions, or domains, within the polymer support in which it is differentially quenched. The fact that the observed quenching sensitivity does not track the measured diffusion coefficient indicates that domains in which the metal complex partitions must exhibit oxygen transport properties dramatically different from the bulk polymer. It is the immediate microenvironment that determines quenching behavior, and this can be quite different from the average bulk properties. An alternative interpretation is that the oxygen solubility is varying greatly with different sample preparations. We cannot exclude this possibility. However, the differences among the preparations are so large and quenching properties of the metal complexes are very sensitive to local conformations. Therefore, we consider solubility variations a less likely interpretation than local microenvironmental differences in *D*.

There are several implications of these results in terms of the rational design of sensors. Most importantly, in the design of sensors that exhibit good quenching, it is the local oxygen transport properties that dictate sensor response. It should be possible to optimize sensor response by tailoring polymer supports such that the local environment of the metal complex is optimized while good bulk diffusion is maintained for quick response.

CONCLUSIONS

The method described here for measurement of *D* for polymer films used as sensor supports is quick and accurate for cast films that exhibit reasonable quenching ($S > 2$). The measurements can be carried out during the course of traditional Stern−Volmer plot determinations by measuring the intensity as a function of time upon introducing a step change in oxygen pressure.

The mathematical model described is more accurate and rigorously correct than those used previously. It is trivial to implement with a conventional quenching apparatus and works well with samples with the higher optical densities required to get good signal-to-noise ratios.

There are some precautions that must be observed to obtain good data. The method does require that the luminophore is uniformly distributed throughout the film. However, this can generally be established by controlling the doping, drying, or polymerization conditions. We have had difficulties with sensor films that exhibit very high quenching and with elastomers. An irregular hump was observed at early times for some highly quenched samples, although reasonable diffusion coefficients can still be obtained. The origins of this artifact are unknown at this time.

Our data demonstrate that the quenching in polymers can be a complex combination of sample preparation and the effects of additives. Quenching behavior can depend critically on the casting solvent. Additives can affect quenching in nonobvious ways. For example, TBP can greatly increase *D* while substantially reducing quenching. This demonstrates that the microenvironment around the sensor molecule is the critical parameter that must be controlled to get good sensing. Given the simplicity of our method for measuring diffusion, it allows workers to readily measure this critical parameter in the same films used for sensing. Since *D* depends so critically on preparation method and materials, *D* should in fact be measured for every film.

ACKNOWLEDGMENT

We gratefully acknowledge support by the National Science Foundation (CHE 97-26999 and 00-94777). K.A.K. acknowledges a Dissertation Year Fellowship from the University of Virginia Department of Chemistry. K.A.K. also recognizes contributions by Louise Sinks.

Received for review August 1, 2001. Accepted November 26, 2001.

AC010867V

(30) Kneas, K. A.; Demas, J. N.; DeGraff B. A.; Periasamy, A. *Microsc. Microanal.* **2000**, *6*, 551−561.

(31) Kneas, K. A.; Demas, J. N.; DeGraff B. A.; Periasamy, A. *Proc. SPIE* **2001**, *4262*, 89−97 (Multiphoton Microscopy in the Biomedical Sciences).

(32) Xu, W.; McDonough, R. C., III; Langsdorf, B.; Demas, J. N.; DeGraff, B. A. *Anal. Chem.* **1994**, *66*, 4133−4141.